Eur. Phys. J. E (2018) **41**: 88
DOI 10.1140/epje/i2018-11698-3

THE EUROPEAN PHYSICAL JOURNAL E

Regular Article

The Daoud and Cotton blob model and the interaction of star-shaped polymers

Albert Johner[1,a] and Nam-Kyung Lee[2,b]

[1] Institut Charles Sadron CNRS, Université de Strasbourg, Rue du Loess, 67034 Strasbourg Cedex 2, France
[2] Department of Physics, Sejong University, Seoul 05006, South Korea

Received 19 April 2018 and Received in final form 27 June 2018
Published online: 25 July 2018

Abstract. Since it was first proposed in 1982, the Daoud and Cotton (DC) model for star-shaped polymers was intensively used also for self-assembled copolymers and small colloids grafted with long polymers. We try to clarify the position of the DC model and focus on the star partition function which plays a central role in self-assembly and gives access to the star-star interaction. While the predicted star-star interaction agrees with scattering data by Likos *et al.* (Phys. Rev. Lett. **80**, 4450 (1998)), an extensive simulation by Hsu *et al.* (Macromolecules, **37**, 4658 (2004)) does not recover the prediction for the partition function. We try to reconcile this seemingly conflicting results. We discuss star-star interactions, star free energy in θ-solvents, mixing of A/B branches in copolymer stars, within or beyond the Daoud and Cotton blob model.

The seminal paper by Daoud and Cotton [1] was primarily motivated by available light scattering and viscosity data acquired for star-shaped polymers (called stars below) in good solvent and aimed at describing the polymer conformations. Shortly after, Witten and Pincus applied the model to describe the interaction between colloids protected by long grafted polymers which were represented as stars [2]. Twelve years later, Likos and Richter put Witten's results to a test by scattering experiments [3] measuring the structure of a semi-dilute star solution. Their conclusion was very appealing, since the predictions from the asymptotic Daoud and Cotton (DC) model were found to apply for functionality $p = 18$ and expected to hold [2] down to functionality $p = 2$, definitively outside the asymptotic regime. The robustness of the DC prediction for the star-star interaction is widely accepted nowadays [4]. An early review on star-shaped polymers [5] discusses experiments and simulations, the latter showing qualitative agreement with the DC model. As a matter of fact, the DC model attracted continuous attention over the past decades underlining the fast growth of soft matter physics and, more recently, of biophysics and medical sciences. Recent citing works deal with star-shaped polymer synthesis [6], star interactions [7,4], branched polymers [8,9], dendrimers [10,11], complexation [12], gels [13], colloids and colloidal crystals [14,15], nanocomposites [16], flow of star-shaped polymer solutions [17], biophysical systems [18,19].

A heroic, and to our knowledge still the most extended, simulation of the star partition function was performed by Hsu, Nadler and Grassberger somewhat later [20]. These data were interpreted as not supporting the DC model. From the start, the DC model had to face renormalization group calculations using ϵ-expansion, ($\epsilon = 4 - d$ with d the dimension of space) [21–24]. As already pointed out by Witten and Pincus, the range of validity of the ϵ-expansion must become narrow as the functionality increases. Nonetheless, in 3d, the ϵ-expansion turns out to give good estimates for $p = 1, 2, \ldots$, but, for large p, the expansion parameter is rather ϵp [23], restricting the domain of application.

The DC model considers stars in the excluded volume regime of high enough functionality for branches to strongly interact and stretch out (fig. 1). In its minimal form, the DC model has the appeal of simplicity. The star corona is seen as a sea of correlation blobs of size ξ increasing when the distance to the star center increases. As showns in fig. 1, the blobs almost do not interpenetrate and are pervaded by one branch each. Adopting the Pincus approximation for brushes where all free branch ends are constrained to lie at the periphery, each sphere of intermediate radius r and area $\sim r^{d-1}$ is bearing p blob sections of area $\xi(r)^{d-1}$, which sets the blob radius $\xi(r) \sim rp^{-1/(d-1)}$. Further neglecting the interaction between blobs, the free energy F in thermal units is obtained

[a] e-mail: albert.johner@ics-cnrs.unistra.fr
[b] e-mail: lee@sejong.ac.kr

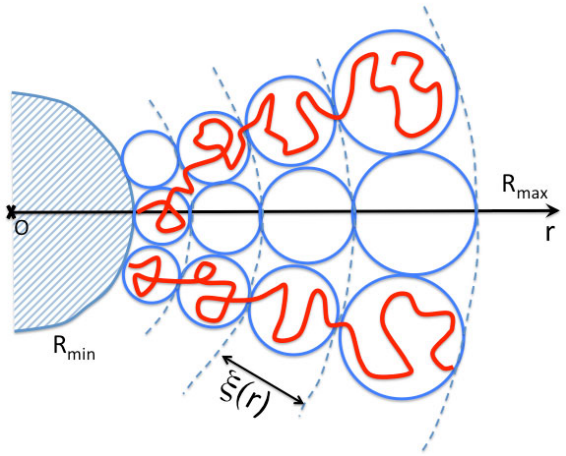

Fig. 1. Two-dimensional sketch of a star within the Daoud and Cotton blob model. The blobs are represented by blue circles with size ξ increasing proportionally to the distance r to the center. Two arm configurations are shown as thick red wavy lines. (Colorized version of the original Daoud and Cotton 1982 drawing.) In the text, the radius $R_{\min}$ of the core (hatched blue) is set to a monomeric size for convenience and its influence not discussed in detail.

by blob counting $F \sim \int_{R_{\min}}^{R_{\max}} p^{d/(d-1)}/r^d \mathrm{d}r^d$. As a result, $F \sim p^{d/(d-1)} \log N$, where $\log R_{\max} \sim \log N$ has been inserted. We recast the free energy and partition function of the DC star as

$$F = \alpha_d p^{\frac{d}{d-1}} \log N; \qquad Z_p = N^{\gamma_p - 1}, \\ \text{with} \qquad \gamma_p - 1 = -\alpha_d p^{\frac{d}{d-1}}, \tag{1}$$

where we adopted the standard notation for the critical exponent of the partition function. We expect the DC model to apply asymptotically for $p \gg 1$. The constant α_d depends on the dimension of space.

The star partition function exponent γ_p has been obtained exactly in 2d, thanks to conformal invariance [22] as $\gamma_p - 1 = (-9p^2 + 27p + 4)/64$. This result is compatible with the 2d DC model, which it supports. It further gives the value $\alpha_2 = 9/64 \approx 0.14$. The 2d results also show a rather sluggish approach of $\gamma_p - 1$ to the DC asymptote which is approached by less than 10% only for $p \geq 18$ (see footnote[1]). At the onset of this regime, the extra free energy per branch (as compared to a free chain) is about $2.3 \log N$ in thermal units. Assuming that α_d is a smooth function of d we expect α_3 to take a value close to α_2.

The field theoretical approach [22] demonstrates a powerful factorization property of the partition function. Following ref. [22], the star partition function factorizes in contributions of its vertices, the central vertex of order (number of legs) p and the peripheral vertices of order 1 for the free ends. Each vertex of order n contributes its vertex exponent σ_n to the star exponent $\gamma_p - 1 = \sigma_p + p\sigma_1$. In 2d the vertex exponents are known exactly

[1] The subdominant (linear in p) term is also divergent and convergence to the asymptote is only seen in log-log scale.

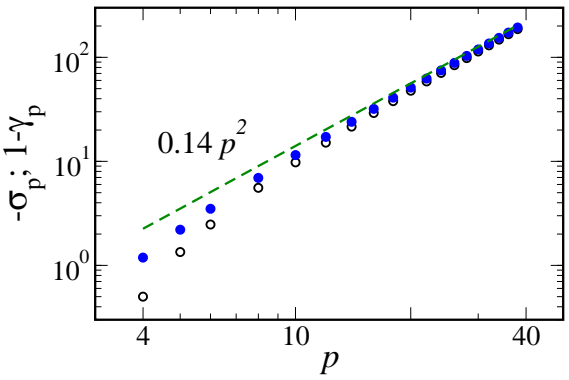

Fig. 2. Daoud and Cotton model in 2d. The plot of the opposite central vertex exponent $-\sigma_p$ and star exponent $-(\gamma_p - 1)$ as a function of the star functionality (number of branches) p in log-scale evidences a common asymptotic power law $(9/64)p^2$. The central vertex exponent (filled symbols) approaches the asymptotic DC law (dashed line) faster than the star exponent (open symbols). The shown values of functionality p range from 4 to 40 for the central vertex exponent.

Table 1. Values of the vertex exponent in 3d, restricted to 3 significant digits, according to the simulation data in ref. [20].

p	1	2	3	4	5	6
σ_p	0.0786	0	−0.193	−0.479	−0.849	−1.29
p	7	8	9	10	12	14
σ_p	−1.80	−2.38	−3.01	−3.71	−5.16	−6.97
p	16	18	20	24	30	40
σ_p	−8.90	−11.0	−13.2	−18.2	−26.8	−43.7
p	50	60	70	80		
σ_p	−64.1	−87.2	−114	−143		

$\sigma_n = (2-n)(9n+2)/64$. The vertex exponent σ_p reaches to the same DC asymptote $-(9/64)p^2$ as the star exponent. It is clear that the DC model ignores the peripheral vertex exponents and rather describes the central vertex. The convergence of the central vertex exponent to the DC is indeed faster, as shown in fig. 2.

Let us now turn to stars in 3d. *A priori* branches see each other less than in 2d and the DC behavior should be shifted to higher functionality than in 2d (where we retained $p \geq 18$). In the absence of exact analytical results, we rely on the simulation data of ref. [20] summarized in table 1.

The central vertex exponent and the star exponent are ploted in fig. 3 as a function of the functionality p in log-log scale. The plot is very similar to the one for 2d in fig. 2. The convergence is again sluggish, more so for the star partition function exponent. As anticipated, higher star functionality is needed to approach the DC limit (for the same 10% criterion, $p > 40$). The approximate determination of the coefficient α_3 (see eq. (1)) from the data gives $\alpha_3 \approx 0.20$ close to the exact value ($9/64 \approx 0.14$) of α_2. In our opinion, the data shown in table 1 support the DC model but demonstrate that high star functionality

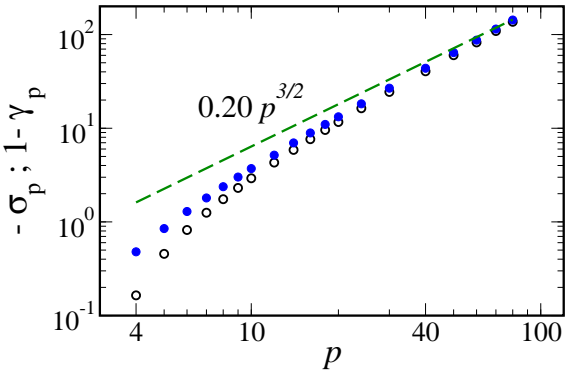

Fig. 3. Daoud and Cotton model in 3d. The plot of the opposite central vertex exponent $-\sigma_p$ and star exponent $-(\gamma_p - 1)$ as a function of the star functionality (number of branches) p in log-scale evidences a common asymptotic power law $0.20p^{3/2}$. The central star exponent (filled symbols) approaches the asymptotic DC law faster than the star exponent (open symbols). The shown functionalities p are: 4, 5, 6, 7, 8, 9, 10, 12, 14, 16, 18, 20, 24, 30, 40, 50, 60, 70, 80. Exponents are taken from the simulation data in ref. [20], see table 1.

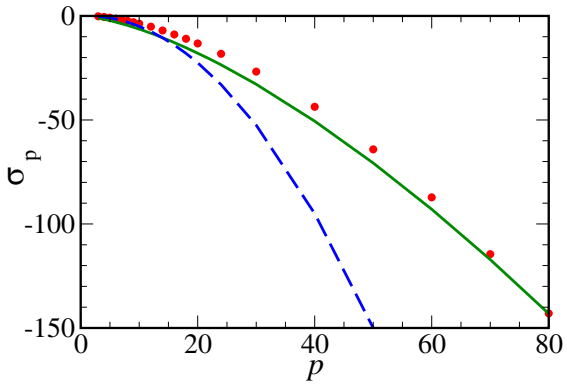

Fig. 4. Daoud and Cotton model *vs.* first-order ϵ-expansion. The plot of the central vertex exponent σ_p as a function of the star functionality (number of branches) p. The first-order ϵ-expansion result is shown (blue dashed line) together with the Daoud and Cotton prediction (green solid line) and simulation data (filled symbols). The first-order RG fits the data at low functionality, while Daoud and Cotton fits at high functionality. The shown functionalities p are: 1, 2, 3, 4, 5, 6, 7, 8, 9, 10, 12, 14, 16, 18, 20, 24, 30, 40, 50, 60, 70, 80. Exponents are taken from the simulation data shown in table 1.

is needed to meet the prediction. For low functionality p, the known RG results must be accurate, we know they are for $p = 2$–4 and the associated contact exponents. As using higher-order ϵ-expansion (without re-summation) is not always helpful we stick to the first-order expansion $\sigma_p = \frac{p(2-p)}{16}\epsilon + \ldots$, where we insert $\epsilon = 1$. Figure 4 indeed shows that the one-loop RG result describes well the data up to $p \sim 5$. Re-summation of the ϵ-series was proposed early by Schäfer [23] for moderate functionality. Some of the obtained values were later successfully compared to simulation data in ref. [20], where the agreement extends to $p = 9$. At this stage it is somehow puzzling that the binary star interaction gained from the DC model was found accurate for all functionalities [3].

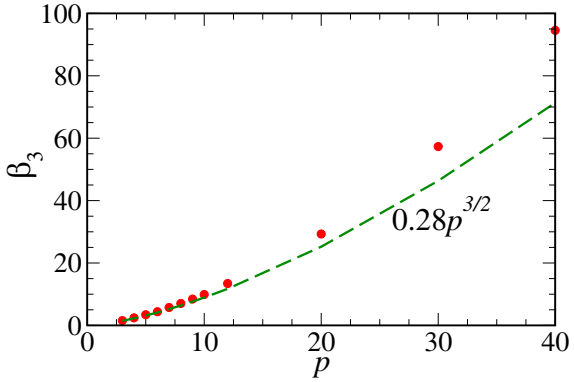

Fig. 5. Interaction between two excluded volume stars. Amplitude of the logarithmic interaction according to the Daoud and Cotton (DC) model (green dashed line) and to the vertex exponents from simulation data (filled symbols). DC performs surprisingly well at low functionality where it should not apply.

A, by now classical, scaling argument relates the partition function of a system of two stars $Z^{(2)}(r)$ with their centers a distance r apart to the partition function of isolated stars. The expression for $Z^{(2)}(r)$ must then crossover smoothly from the product of the single star partition functions for distant non-interacting stars ($r > 2R$) to the partition function of a star cumulating the branches of both stars when their centers (almost) coincide. Specializing to two identical stars, $Z^{(2)}(r) \sim Z_p^2 \times (\frac{r}{R})^x$, where the power x is fixed by the condition, $Z^{(2)}(b) \sim Z_{2p}$, with b a monomeric size (to keep things simple). Assuming $R \propto N^\nu b$ with ν the swelling exponent (in 3d $\nu \approx 0.588$), where powers of p are neglected, we arrive at $x = (2\sigma_p - \sigma_{2p})/\nu$. This corresponds to the repulsive effective pair potential:

$$U = -k_B T \frac{2\sigma_p - \sigma_{2p}}{\nu} \log \frac{r}{R}, \quad \text{for } r \ll R. \qquad (2)$$

The extreme case $r \sim b$ is relevant to the barrier opposing star fusion [25]. We will come back to intermediate lengthscales and refinements at low compression below. For stars in the DC limit the amplitude $\beta_d = \frac{2\sigma_p - \sigma_{2p}}{\nu}$ of the potential in eq. (2) simplifies to $\tilde{\beta}_d p^{d/(d-1)}$ with $\tilde{\beta}_d = \alpha_d(-2 + 2^{d/(d-1)})/\nu$, which evaluates to $\tilde{\beta}_3 = 0.28$ (3d) and to $\tilde{\beta}_2 = 3/8 \approx 0.37$ (2d). The amplitude of the interaction is plotted in fig. 5 against the functionality p according to the 3d simulation data shown in table 1. The highest accessible functionality is $p = 40$ ($2p = 80$). The DC prediction for interactions works quite well at low functionality, where DC does not work for the star partition function itself. The reason is that the difference of the data for σ_p (table 1) and the DC estimate is almost linear in p between $p = 1$ and $p = 20$, tentatively $\sigma_p \approx -\alpha_3(p^{3/2} - \sqrt{2}p)$, which satisfies $\sigma_2 = 0$, as is shown in fig. 6[2]. A linear in p contribution to σ_p is not relevant to

[2] We do not have any deep argument for this heuristic expression. A linear in functionality p correction to the DC model

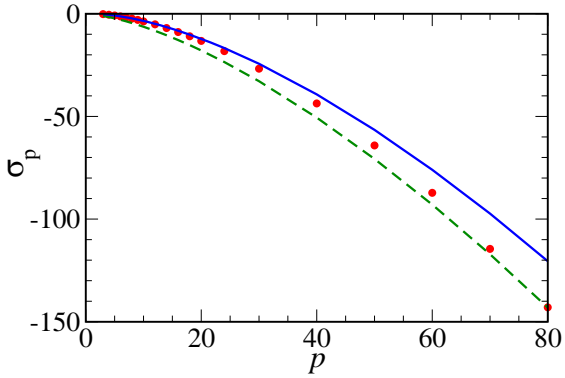

Fig. 6. Simulation data for the vertex exponent after ref. [20] (filled symbols) compared to the Daoud and Cotton prediction (green dashed line) and to the empirical formula adding a linear in functionality term to the DC prediction so as to match $\sigma_2 = 0$ (blue solid line). The fair accuracy of the empirical formula rationalizes the success of the DC prediction for the interaction for stars of low functionality outside the DC limit for the partition function.

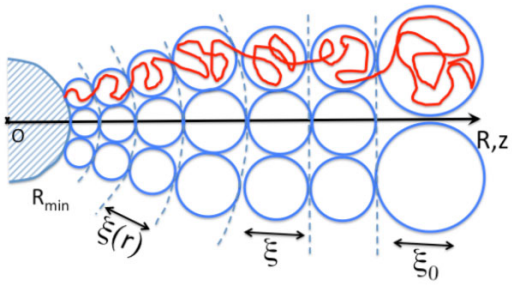

Fig. 7. Daoud and Cotton blob model augmented by the almost flat outer corona. The outer flat corona corresponds to a grafting distance ξ between chains. The polymer concentration is quantitatively decreasing with the height z, which goes beyond the standard (DC-like) Pincus blob model. For simplicity, the flat brush is shown with uniform blob size, except for the outermost ones. Unlike in the standard blob model, not all branches participate in the outermost blob layer. Those branches reaching there are quantitatively more stretched in the core of the brush. The correlation lengths $\xi(r)$, ξ and ξ_0 introduced in the text are shown.

the interaction. There is a pretty large regime where DC is inaccurate for the interaction, essentially because σ_p and σ_{2p} do not follow the same law (fig. 6). The above scaling argument implicitly assumes that there is no other length scale in the problem than the star radius R, or at least that "compression" goes beyond any other intermediate length scale.

Triplet interactions were found generally attractive but of lesser importance [26].

At this stage it must be noted that an alternative approach to the pair interaction, which complements eq. (2) and seems suited for the interaction of stars in semi-dilute solutions where stars overlap, has been built from the star structure according to the DC model. The main idea there is that curvature is almost irrelevant in the, say, outer half of the star [27] (fig. 7).

The pair interaction is obtained from the structure of the stars and the interaction of the equivalent flat grafted layers [28], which is not captured by the DC model. The largest correlation length in the DC blob construction $\xi = R/\sqrt{p}$ now characterizes the outer flat polymer brush of grafting density $1/\xi^2$. The (much) larger correlation length ξ_0 characterizes the outer edge of the equivalent flat brush. According to the strong stretching theory for excluded volume brushes [28] and to its correction for edge fluctuations $\xi_0 \sim N^{2\nu/3}\xi^{1/3}$, altogether this leads to the correlation length in the star edge $\xi_0 \sim \xi p^{\nu/3} \sim Rp^{-1/2+\nu/3}$. When two flat brushes are moderately pushed against each other, they barely overlap much less than the reduction of their distance beyond contact and merely compress. (There is no interpenetration at all in the strict strong stretching limit.) The compression energy per unit area has been obtained in ref. [28] as

$$F_{flat} \sim \xi_0^{-2}(\Delta h/\xi_0)^{(3+4\nu)/(3-2\nu)},$$

for a reduction of distance Δh beyond contact. The total repulsion between stars, which interact over an area $A \sim R\Delta h$, reads

$$U \sim p^{\frac{3-2\nu}{6}}\left(\frac{\Delta h}{\xi_0}\right)^{\frac{6+2\nu}{3-2\nu}} \sim p^{3/2}\left(\frac{\Delta h}{R}\right)^{\frac{6+2\nu}{3-2\nu}}. \qquad (3)$$

This expression applies for $\xi_0 < \Delta h < R$ and provides a smooth transition between an interaction A/ξ_0^2 for $\Delta h \sim \xi_0$ and $p^{3/2}$ for $\Delta h \sim R$. The later is compatible with eq. (2). Equations (2) and (3) provide a scaling description of the pair interaction over the whole compression regime within the DC limit. As a matter of fact, the external blob size ξ_0 is rather large $\xi_0 \sim Rp^{-1/2+\nu/3}$, where the exponent is close to -0.304. The intermediate regime described by eq. (3) only extends over a factor ≈ 3 in Δh for $p = 40$, but the interaction steeply increases, roughly as $(\Delta h)^{3.9}$ by a factor ≈ 79. Experiments on semi-dilute star solutions should detect the intermediate regime eq. (3) close to the overlap concentration. While deeper in the semi-dilute regime the scaling result (eq. (2)) should apply with its DC form being accurate at both low and high functionalities. As explained earlier the success of the DC result at low functionality might be a bit fortuitous.

A remarkable feature of the DC model is that the exponent of the partition function and the central vertex exponent only depend on the dimension of space. In particular, their derivation is independent of the quality of the solvent. (The star radius R does of course depend on the quality of the solvent.) As a matter of fact, the same power law behavior of the partition function is obtained at the θ-temperature taken here as the temperature, where the effective two-body interactions vanish,

$$F_p^\theta \sim p^{3/2}\log N \quad \text{(DC at the } \theta\text{-point)}. \qquad (4)$$

may perhaps arise, for example, from the free end distribution entropy, but cannot be retained here as it does not fit for large p values.

As noted previously [29], this is at odds with the available RG result [22] $F_p^\theta \propto p^3 \log(\log N)$. We reached the conclusion that the RG result describes stars with unstretched arms and applies for $\log N \gg p^2$ (either exponentially long branches or low functionality) while the DC type of result describes somewhat crowded stars with stretched branches and applies for higher functionality and moderately long branches (the typical case). A slightly augmented result [29] explicitly accounts for the renormalized three body interaction,

$$F_p^\theta \sim p^{3/2} \frac{\log N}{(1+\kappa \log N)^{1/4}}\,, \tag{5}$$

where the Ginzburg parameter κ measures the strength of the three body interaction[3]. Equation (5) for the free energy describes stars with stretched branches. It differs from the DC by a logarithmic factor and matches DC in the mean-field regime (small κ). Equation (5) applies for moderate branch length/high functionality up to $\log N \sim p^2$ where it crosses over to the critical regime (RG) with unstretched branches, for $\kappa \log N \gg 1$ with $\log(\log N)$ replaced by 1. The above relies on local microscopic monomer-monomer interactions, pseudo-potentials (δ-potentials). There are corrections to eq. (5) from higher moments of the microscopic potential other than its volume integral. For details see ref. [29].

Over the last decades the Self-Consistent Mean-Field (SCMF) theory was developed and was successfully applied to describe weakly fluctuating polymer-phases (or meso-phases). The sometimes analytically tractable strong stretching limit of it [30,31] comes very close to the DC model in spherical (or cylindrical) symmetry. In the strong stretching limit [30–32] the polymer configuration is uniquely defined by its end position(s) and the end distribution becomes the main ingredient of the theory. For star-shaped polymers free chain ends are totally excluded from the vicinity of the center in the strong stretching approximation, which makes the problem difficult and only approximate solutions are known. The exclusion zone problem has been explicitly addressed in cylindrical geometry [33].

Recent theoretical work also addresses stars with two type of branches differing by chemistry (fig. 8). This is directly linked to the polymer-A/polymer-B/solvent ternary mixture problem [34] which turns out pretty rich. The case where both polymers are in a common good solvent but repel each other can also be considered in the DC model and local A/B separation can be studied. As blobs almost do not interpenetrate, the A/B interaction is drastically reduced. The number of contacts between neighboring A and B blobs of monomer content $g \sim \xi^{1/\nu}$, reads $\sim (g/\xi^3) g g^{\sigma_4}$ and involves the vertex exponent $\sigma_4 \approx -0.479$ [20], which accounts for the fraction of inter blob contacts. Let χ be the interaction between A/B monomers. The interaction between A/B

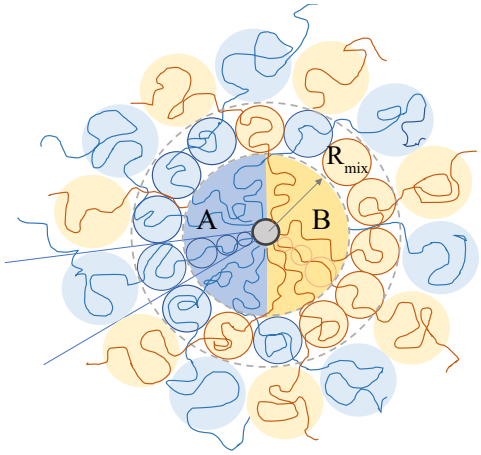

Fig. 8. Schematics of a star with two types of branches: A and B, which are represented as blue and orange. Branches are separated closer to the center and mix beyond $R_{\rm mix}$.

blobs can be written as $\chi g^{-\chi_s}$ [34], with the exponent[4] $\chi_s = 3\nu - \sigma_4 - 2 \approx 0.243$. As the integral of the A/B interaction between blobs over the homogeneous DC star $F_{\rm A/B}$ is dominated by the vicinity of the center, it has no N dependence but a large p dependence:

$$F_{\rm A/B} \sim \chi \phi_{\rm A} \phi_{\rm B} p^{3/2+\chi_s/(2\nu)} \left(\frac{R_{\rm min}}{b}\right)^{-\chi_s/\nu}\,, \tag{6}$$

where $\phi_{\rm A(B)} = p_{\rm A(B)}/(p_{\rm A}+p_{\rm B})$ is the fraction of A(B) branches. Within the DC regime, the expression of $F_{\rm A/B}$ essentially depends on the functionality. ($R_{\rm min}$ may be microscopic $\sim b$.) The critical χ-parameter $\chi^\star$ is defined by $F_{\rm A/B}/p \approx 1$, more precisely $\chi^\star p^{1/2+\chi_s/(2\nu)} R_{\rm min}^{-\chi_s/\nu} \sim 1$. The exponent of p has two contributions: the first term (1/2) accounts for the number of blobs per arm within a scale of $R_{\rm min}$, and the second term stands for the contribution of the A/B interaction per blob. Separation between antagonistic branches of A- and B-type stars at the center and extends outward for increasing χ. Assuming mixed A/B branches beyond the crossover distance $R_{\rm mix}$ from the center,

$$\chi p^{1/2+\chi_s/(2\nu)} R_{\rm mix}^{-\chi_s/\nu} \sim 1,$$

holds ($R_{\rm mix} \geq R_{\rm min}$ by construction). Finally separation affects the whole star for $R_{\rm mix} = R_{\rm max}$, where the star radius is given by $R_{\rm max} = N^\nu p^{1/2-\nu/2}$.

There is extended work by von Ferber [35] on the field theoretical side exploring all fixed points of ref. [34]. The main output is the vertex exponent $\sigma(p_{\rm A}, p_{\rm B})$ for a star with $p_{\rm A,B}$ branches of type A, B at all fixed points (common good solvent and mutual repulsion, common theta solvent and mutual repulsion, ...). As such, without resummation, the results are valid in 3d for $p \sim 1$ and complement the DC model. Long-range, power law, correlated structural disorder can change the universality class

[3] The Ginzburg parameter $\kappa = 22 a_3/(2\pi)^2$ only depends on the dimensional effective third virial coefficient a_3.

[4] The seminal paper [34] does not give the simple scaling argument but provides a strictly equivalent expression involving a less transparent critical exponent.

of polymers. Stars in random media were considered recently and the influence of long-range correlated disorder analyzed [36].

Star adsorption on a flat interface can be considered within the DC model. Single star adsorption was analyzed by Halperin and Joanny [37]. There it is shown how the star progressively flattens for increasing adsorption strength. In the intermediate state the star takes a sombrero shape where the free star structure is retained close to the center. The authors fail to describe the plateau of the isotherm. A more recent mean-field theory on adsorption of branched polymers does not exhaust the problem [38]. It would be worthwhile to try and apply our increased knowledge on adsorption layers to this problem.

Considerable efforts were put in the elucidation of the star structure [5] both in dilute and semi-dilute or concentrated solutions. Neutron scattering [5,39] and X-ray scattering [40] have been used intensively. In parallel, models, usually derived from DC, were developed [41,42,39]. The form factor of linear chains in the critical excluded volume regime turns out to be rather complicated [43] and involves des Cloizeaux contact exponents. The same holds true for excluded volume stars of low functionality. Even in the DC limit, some intra-blob/inter-blob contributions do involve contact exponents (see above for the inter-blob contacts).

In this short paper, we tried to clarify the position of the Daoud and Cotton model for star polymers. The DC model has been often underestimated by theorists from the very beginning. In contrast, its simplicity attracted a lot of attention from experimentalists. Many experiments, a few of which are cited in this paper, found that the DC model performs well, sometimes outside its expected range of validity. There is a substantial correction to the vertex exponent from the DC model at low functionality. The correction is almost linear in functionality and cancels out in the interaction. This explains the success of the DC model for the interaction at low functionality. The linear in functionality correction to DC should not be confused with an asymptotic correction valid at high functionality, as is the case in 2d. There is a wide intermediate regime where the star under consideration and the star with double functionality do not follow the same law and the DC prediction for the interaction is inaccurate (between $p = 20$ and $p \sim 60$, the upper limit is not precise from the data). The available data for the vertex can be tentatively fitted by the DC type of formula $\sigma_p = \alpha_3 p^{3/2}$ with $\alpha_3 \approx 0.20$ for $p \geq 50$ and the heuristic formula $\sigma_p = \alpha_3(p^{3/2} - \sqrt{2}p)$, enforcing $\sigma_2 = 0$, for $p \leq 20$, both of which lead to the pair interaction $U = \beta_3 p^{3/2} \log(R/r)$ with $\beta_3 = 0.28$, for a distance between centers r much smaller than the star radius R ($r \ll R$). The DC model, or simple variants of it, also allows to discuss separation in copolymer stars. For A/B copolymer stars with homogeneous branches we predict separation of A/B branches closer to the center and mixing of branches in an outer corona, see fig. 8. The DC model also applies to stars in θ-solvent where it is predicted to perform better than available RG results but for low functionality or exponentially large branches.

Finally the scattering function of stars or solutions of stars can also be described in the DC model. Its expression usually involves the swelling exponent ν. We suggest that it should also contain vertex exponents like σ_4 or the associated contact exponents introduced by des Cloizeaux [21].

This work originated from discussions with M. Daoud. We would like to dedicate it to the memory of Jean-Pierre Cotton.

Author contribution statement

Both authors contributed equally to this work.

References

1. M. Daoud, J.P. Cotton, J. Phys. (Paris) **43**, 531 (1982).
2. T.A. Witten, P.A. Pincus, Macromolecules **19**, 2509 (1986).
3. C.N. Likos, H. Löwen, M. Watzlawek, B. Abbas, O. Jucknischke, J. Allgaier, D. Richter, Phys. Rev. Lett. **80**, 4450 (1998).
4. M. Benhamou, M. Himmi, H. Kaidi, J. Mol. Liq. **230**, 337 (2017).
5. G. Grest, L. Fetters, J. Huang, D. Richter, Adv. Chem. Phys. **94**, 67 (1996).
6. R. Whitfield, A. Anastasaki, N.P. Truong, P. Wilson, K. Kempe, J.A. Burns, T.P. Davis, D.M. Haddleton, Macromolecules **49**, 8914 (2016).
7. X. Lang, W.R. Lenart, J.E.P. Sun, B. Hammouda, M.J.A. Hore, Macromolecules **50**, 2145 (2017).
8. R. Everaers, A.Y. Grosberg, M. Rubinstein, A. Rosa, Soft Matter **13**, 1223 (2017).
9. R. Hu, D.T. Wu, Phys. Rev. E **95**, 042502 (2017).
10. I.O. Lebedeva, E.B. Zhulina, F.A.M. Leermakers, O.V. Borisov, Langmuir **33**, 1315 (2017).
11. M. Wengenmayr, R. Dockhorn, J.U. Sommer, Macromolecules **49**, 9215 (2016).
12. P. Hebbeker, A.A. Steinschulte, S. Schneider, J. Okuda, M. Moeller, F.A. Plamper, S. Schneider, Macromolecules **49**, 8748 (2016).
13. O. Rud, T. Richter, O. Borisov, C. Holm, P. Kosovan, Soft Matter **13**, 3264 (2017).
14. H. Zhang, W. Wang, S. Mallapragada, A. Travesset, D. Vaknin, Nanoscale **9**, 164 (2017).
15. X.W. Gu, X. Ye, D.M. Koshy, S. Vachhani, P. Hosemann, A.P. Alivisatos, Proc. Natl. Acad. Sci. U.S.A. **114**, 2836 (2017).
16. T. Krentz, M.M. Khani, M. Bell, B.C. Benicewicz, J.K. Nelson, S. Zhao, H. Hillborg, L.S. Schadler, J. Appl. Polym. Sci. **134**, 44347 (2017).
17. V.R. Ahuja, J. van der Gucht, W.J. Briels, J. Chem. Phys. **145**, 194903 (2016).
18. J. Irianto, Y. Xia, C.R. Pfeifer, R.A. Greenberg, D.E. Discher, Biophys. J. **112**, 446 (2017).
19. N. Giamblanco, G. Marletta, A. Graillot, N. Bia, C. Loubat, J.F. Berret, ACS OMEGA **2**, 1309 (2017).
20. H.P. Hsu, W. Nadler, P. Grassberger, Macromolecules **37**, 4658 (2004).
21. J. des Cloizeaux, G. Jannink, *Polymers in Solution* (Oxford University Press, Oxford, 1990).
22. B. Duplantier, J. Stat. Phys. **54**, 581 (1989).

23. L. Schäfer, C. von Ferber, U. Lehr, B. Duplantier, Nucl. Phys. B **374**, 473 (1992).
24. V. Schulte-Frohlinde, Y. Holovatch, C. von Ferber, A. Blumen, Phys. Lett. A **328**, 335 (2004).
25. N.K. Lee, C. Abrams, J. Chem. Phys. **121**, 7484 (2004).
26. C. von Ferber, A. Jusufi, C.N. Likos, H. Löwen, M. Watzlawek, Eur. Phys. J. E **2**, 311 (2000).
27. A.N. Semenov, J.F. Joanny, A.R. Khokhlov, Macromolecules **28**, 1066 (1995).
28. S.T. Milner, T.A. Witten, M.E. Cates, Macromolecules **21**, 2610 (1988).
29. A. Johner, EPL **96**, 46004 (2011).
30. A.N. Semenov, Sov. Phys. JETP **61**, 733 (1985).
31. Y.B. Zhulina, V.A. Pryamitsin, O.V. Borisov, Polym. Sci. U.S.S.R. **31**, 205 (1989).
32. S.T. Milner, T.A. Witten, M.E. Cates, Europhys. Lett. **5**, 413 (1988).
33. R.C. Ball, J.F. Marko, S.T. Milner, T.A. Witten, Macromolecules **24**, 693 (1991).
34. J.F. Joanny, L. Leibler, R. Ball, J. Chem. Phys. **81**, 4640 (1984).
35. C. von Ferber, Y. Holovatch, Phys. Rev. E **56**, 6370 (1997).
36. V. Blavatska, C. von Ferber, Y. Holovatch, Condens. Matter Phys. **15**, 33603 (2012).
37. A. Halperin, J.F. Joanny, J. Phys. II **1**, 623 (1991).
38. A. Johner, J.F. Joanny, J. Phys. II **6**, 511 (1996).
39. G. Volet, L. Auvray, C. Amiel, J. Phys. Chem. B **113**, 13536 (2009).
40. G.M.E. Pozza, S. Crotty, M. Rawiso, U.S. Schubert, P.J. Lutz, J. Phys. Chem. B **119**, 1669 (2015).
41. C.M. Marques, D. Izzo, T. Charitat, E. Mendes, Eur. Phys. J. B **3**, 353 (1998).
42. L. Auvray, private communication. About at the same time as ref. [41] was worked out, Loïc Auvray circulated a calculation of the structure factor. It is in particular cited in ref. [40].
43. A. Johner, H. Benoit, J.F. Joanny, Makromol. Chem. Theory Simul. **4**, 45 (1995).